Journal of Energy Storage 55 (2022) 105563

Contents lists available at ScienceDirect

Journal of Energy Storage

journal homepage: www.elsevier.com/locate/est

Research papers

Storage-integrated virtual power plants for resiliency enhancement of smart distribution systems

Ghasem Piltan [a], Sasan Pirouzi [b], Alireza Azarhooshang [c], Ahmad Rezaee Jordehi [d,*], Ali Paeizi [e], Mojtaba Ghadamyari [e,f]

[a] Department of Electrical Engineering, Malayer University, Malayer, Iran
[b] Power System Group, Semirom Branch, Islamic Azad University, Semirom, Iran
[c] Department of Electrical and Electronics Engineering, Shahid Beheshti University, Tehran, Iran
[d] Department of Electrical Engineering, Rasht Branch, Islamic Azad University, Rasht, Iran
[e] Department of Electrical Engineering, Shahid Beheshti University, Tehran, Iran
[f] Department of Computer Engineering, Lebanese French University, Kurdistan Region, Iraq

ARTICLE INFO

Keywords:
Storage systems
Electric vehicles
Adaptive robust optimization
Resiliency
Distribution network
Virtual power plant

ABSTRACT

With emergence of Flexible Renewable Virtual Power Plants (FRVPPs) as the aggregator of renewable energy systems and flexibility resources such as demand response programs and electric vehicles (EVs) in the Smart Distribution Network (SDN), FRVPPs are expected to have significant capability resiliency enhancement against natural disasters. This paper focuses on the resilient operation of SDN influenced by FRVPPs for flood and earthquake conditions and minimizes the total cost of the SDN against natural disasters. The constraints of the problem include AC optimal power flow equations, resiliency constraints and FRVPP constraints. The uncertainties of load, energy prices, renewable power generation, EVs demand, accessibility of SDN devices and FRVPP components are modeled using a hybrid stochastic-robust strategy. A hybrid metaheuristic optimization algorithm, based on combination of krill herd optimization and sine-cosine algorithm, has been used to solve the proposed optimization model. The achieved results on the IEEE 69-bus SDN approve the significant capability of FRVPP's in improving the resiliency of the SDN against flood and earthquake. Based on the simulation results, the mentioned hybrid algorithm is capable of extracting the optimal point in lower computing time compared to non-hybrid algorithms. Its standard deviation in the final response is very low, around 0.93 %, which means that the above-mentioned solver extracts an almost unique solution. In addition, the proposed design with energy management of FRVPPs has been able to improve resilience by about 95 % compared to power flow studies. This number is about 33 % and 42 % to improve the state of energy loss and voltage profile, respectively. Of course, these characteristics obtained for FRVPP are the result of the optimal performance of mobile energy storage (EVs) along with the demand response program.

1. Introduction

1.1. Motivation

Renewable energy sources (RESs) are promising solutions to power systems [1], particularly for distribution systems, to provide clean energy [2]. Because RESs are a source of uncertainty [3], it is expected that the results of day-ahead and real-time operations differ [4] because of a prediction error in the RES output energy [5]. From the electricity market point of view, this will pose costs for the network during day-ahead and real-time operations [6]. From a technical perspective, it also refers to the low flexibility [7]. A general definition of flexibility is "*modifying the generation injection and/or consumption paths in a reaction to the external price or activation signal to procure a service in the electrical system*" [8]. To improve this situation, it is necessary to utilize flexibility resources alongside RESs [9]. Since EVs and demand response programs (DRPs) are owned by energy consumers [10], i.e., EVs and DRPs are distributed at consumption points, and their time constants are low, these elements are desirable sources of flexibility [11]. Moreover, the presence of sources and active loads (ALs), i.e., EVs and DRPs, dispersed across the distribution system reduces the rate of power outages during faults in this system, such as the outage of distribution lines due to floods or earthquakes [12]. The reason is that in these conditions, local sources

* Corresponding author.
E-mail addresses: s.pirouzi@iau.ac.ir (S. Pirouzi), ahmadrezaeejordehi@gmail.com (A. Rezaee Jordehi), mojtaba.Ghadamyari@lfu.edu.krd (M. Ghadamyari).

https://doi.org/10.1016/j.est.2022.105563
Received 8 June 2022; Received in revised form 20 August 2022; Accepted 26 August 2022
Available online 6 September 2022

Nomenclature

Indices and sets

j	Bus index
n, v, t, s	Indices of bus, FRVPP, hour, and scenario
ref	Slack bus
$\Lambda_N, \Lambda_{VPP}, \Lambda_T, \Lambda_S$	Sets of buses, FRVPPs, hours, and scenarios

Variables

$Cost$	The total expected costs of operation and resiliency ($)
CR^u, DR^u	Uncertainty variable related to charge and discharge rates of EVs placed in FRVPPs (p.u.)
$EENS$	Expected energy not-supplied (p.u.)
E^{uArr}, E^{uDep}	Uncertainty variable for arrival and departure energies of EVs placed in FRVPPs (p.u.)
P^{DIS}, P^{CH}, Q^{EV}	Active power of battery charging and discharging of EVs and reactive power of charger of EVs (p.u.)
P^{DL}, Q^{DL}	Active and reactive power flowing through the distribution line (p.u.)
P^{DR}	Active power of DRP (p.u.)
P^{DS}, Q^{DS}	Active and reactive power of the distribution substation (p.u.)
P^{NS}	Load not-supplied (p.u.)
P^{PV}, Q^{PV}	Active and reactive power of the photovoltaics (PVs) (p.u.)
P^u, Q^u	Uncertainty variable related to active and reactive load (p.u.)
$\overline{P}^{uPV}, \overline{P}^{uW}$	Uncertainty variable related to active power generation by PVs and wind turbines (WTs) in p.u.
P^V, Q^V	Active and reactive power of FRVPP (p.u.)
P^W, Q^W	Active and reactive power of WTs (p.u.)
$\overline{S}^{uEV}$	Uncertainty variable related to charger capacity of EVs in FRVPP (p.u.)
V, ϕ	Voltage magnitude (p.u.) and phase angle (rad)
x	A binary variable related to charging and discharging operation modes of EVs in FRVPP
λ^u	Uncertainty variable related to energy price ($/MWh)

Constants

A, B	Incidence matrix of buses and FRVPP, and incidence matrix of buses and distribution lines
CR, DR	Charge and discharge rates of EVs (p.u.)
E^{Arr}, E^{Dep}	Arrival and departure energies of EVs (p.u.)
g, b	Conductance and susceptance of distribution line (p.u.)
P^L, Q^L	Active and reactive load (p.u.)
$\overline{P}^{PV}, \overline{P}^{W}$	Maximum active power generation by PVs and WTs concerning weather conditions (p.u.)
$\overline{S}^{DL}, \overline{S}^{DS}$	The size of distribution line and substation (p.u.)
$\overline{S}^{EV}$	Size of EV charger (p.u.)
$\overline{S}^{PV}, \overline{S}^{W}$	Size of PVs and WTs (p.u.)
$u^{DL}, u^{DS}, u^{PV}, u^W, u^{EV}$	Availability of distribution line and substation, PVs, WTs, and EVs parking lot
$\underline{V}, \overline{V}$	Minimum and maximum voltage magnitude (p.u.)
$VOLL$	Value of the lost load ($/MWh)
V_{ref}	The voltage magnitude of the slack bus
γ	The participation rate of customers in the DRP
η^{DIS}, η^{CH}	Charge and discharge efficiency of EVs battery
λ	Energy price ($/MWh)
π	Probability of occurrence of a scenario

can supply part of the network consumers. In other words, it is predicted that the distribution of sources and ALs at the network level may dramatically impact the resiliency enhancement of the distribution system against natural disasters [63]. However, it should be noted that all the mentioned advantages require proper management of these elements in the network, which is one of the requirements for the management of these elements by an aggregator such as the virtual power plants (VPPs) [13]. It is further expected that by suitably coordinating VPPs and distribution system operators (DSOs) a suitable energy management system is provided [14], besides improving the network operation indices [15], the resiliency of the network during natural disasters can be enhanced.

1.2. Literature review

The literature thoroughly discusses the optimal operation of VPPs. In [16], the authors analyze the participation of flexible VPPs including photovoltaics (PV), hydro sources, and pumped storage in the energy market. Thus, it presents a two-stage problem, to evaluates the participation of VPPs in the market, and consider the power correction model based on the limitations of irradiation, regional water status, and environmental constraints for VPPs. Referring to the results obtained in [16], the VPP can store energy, supply clean energy, and provide system flexibility. In [17], the VPP consists of traditional generation units, energy storage, responsive loads, and wind systems, where the first element is considered as the flexibility source of the wind system. Proper management of these sources in the VPP helps to participation of these sources in the ancillary services market, such as reserve regulation, besides participation in the energy market. This is commensurate with the promotion of its financial benefit in the electricity market [17]. Active distribution network operation influenced by VPPs is investigated in [18], which presents a bilevel problem for this purpose. The upper-level problem considers active distribution network operation to minimizes the operating costs, while the lower-level problem deals with the VPP operation to maximize its profit and thus provide ancillary services. As per the results [18], VPP is a suitable solution to enhance economic and operation indices including voltage profile and energy loss in the distribution network by controlling its active and reactive power. The same scheme has been implemented in [19], except that it considers the presence of thermal energy consumers in addition to electrical energy consumers in the VPP. Then, according to [19], VPPs enhance the network operation indices by coordinating their operator, various sources, and storage devices. In [20], the authors adopt a two-layer energy management system to manage smart distribution network (SDN) influenced by VPPs. In the first layer, VPP operator is coordinated with sources and ALs in the VPP, while the coordination of the VPP operator with the DSO is dealt with in the second layer. It then presents a bilevel optimization problem. The upper-level problem models the VPP participation in the energy market, while the SDN operation is presented in the lower-level problem. The same results as [18,19] are obtained in [20]. In [21], proper management of the VPP in an unbalanced distribution network reduces the unbalance of the system. The capability of VPPs in regulating the distribution network voltage is investigated in [22], where it is observed that VPPs are capable of controlling active and reactive power of their sources as well as ALs, thus play an effective role in voltage regulation of the distribution system.

A VPP energy management system based on blockchain is proposed in [23] so that energy activities between residential customers is facilitated using renewable energy sources, storage devices, and flexible demand in the VPP. More importantly, end-users are able to successfully send and receive energy so that they economically benefit while using services, including feed-in energy, energy reserve, and demand response, with the help of the VPP. A decentralized optimization algorithm has also been introduced to respect independency and privacy of

end-users by optimizing their energy scheduling, trade, and services. The authors also design a sample blockchain network to manage energy in the VPP and apply the suggested algorithm to this network. Another interesting design is proposed in [24], in which a VPP operating based on renewable energy sources is adopted. The VPP, in this study, operates together with probabilistic wind and solar units, non-renewable distributed generation (DG) units, and dispatchable loads. To enhance efficiency in terms of economic, the VPP's operation scheduling is optimized in a market. In another study, the authors [25] suggest an optimal bidding strategy for VPPs that are involved in energy markets. Ref. [26] categorize renewable power, electricity price in the market, and the demand level as the basic uncertain parameters. According to this, the required formulations are structured while presenting the optimization expressions including objective functions and constraints with the ultimate aim of improving the performance of VPPs subject to some uncertain factors.

As observed in [16–22], VPPs suitably manage their sources active and reactive power, while ALs can improve the technical characteristics of the network such as operation, security, and reliability. Nonetheless, most research studies investigate improving performance indicators including voltage profile and energy loss by VPPs. Yet, since VPPs are distributed across the network, they can be considered as local sources in the power system. Consequently, it is possible that VPPs can reduce the rate of blackouts or enhance network resiliency in the occurrence of N − k contingency caused by natural disasters. However, rarely has this been focused on in the literature. In general, to enhance the resiliency of the distribution network, the literature proposes the establishment of hardening sources and equipment in the network. As in [27], the construction of hardening distribution lines, tie lines, and synchronous distributed generations (SDGs) as well as the use of a system reconfiguration plan in the distribution network is presented for resiliency enhancement. This plan is also presented in [28], except that it provides a robust model for the said plan that can achieve the mentioned planning in the worst-case scenario resulting from uncertainties of energy price and loads. Moreover, to eliminate the construction cost of sources and equipment to improve system resiliency, only the reconfiguration potential of the system to enhance system resiliency against natural disasters has been investigated in [29]. Reconfiguration can reduce the rate of blackouts in critical situations by taking the right path between the distribution substation and customers. In [30], the effects of power electronics and energy storage devices are considered in enhancing network resiliency. In the end, Table 1 lists a summary of the literature.

Table 1
A summary of the literature.

Ref.	Investigate VPP impacts on SDN resiliency	Obtain flexible VPP using customer devices, i.e. DRP and EVs	Solver
[16]	No	No	NHEA
[17]	No	No	MA
[18]	No	No	LAM
[19]	No	No	LAM
[20]	No	Yes	LAM
[21]	No	No	MA
[22]	No	No	MA
[23]	No	No	MA
[24]	No	No	MA
[25]	No	No	MA
[26]	No	No	AM
[27]	No	No	LAM
[28]	No	No	LAM
[29]	No	No	MA
[30]	No	No	MA
PM	Yes	Yes	HMA

PM: Proposed model, MA: Math metical approach, LAM: Linear approximation method, NHEA: Non-hybrid hybrid algorithm, HMA: Hybrid meta-heuristic algorithm.

1.3. Research gaps

According to the above description of the literature (summarized in Table 1), the study on resiliency enhancement of distribution networks influenced by VPPs lack some considerations as given below:

- Most research utilizes hardening equipment such as distribution lines and substations and SDGs to improve the resiliency of the distribution network against natural disasters. Note, however, that due to the low pollution levels of RESs and EVs, the presence of these elements in the network is expected to grow significantly in the near future. Also, their coordination in the framework of VPP can bring technical advantages such as achieving high flexibility and a favorable economy for the mentioned elements [20]. Additionally, due to the distribution of these VPPs at the distribution network level, it is predicted that they will reduce the frequency of consumer interruptions in the event of natural disasters. In other words, VPP can help improve distribution network resiliency. Nevertheless, this has rarely been examined in the literature. Note, however, that since VPPs are owned by energy consumers, energy customers can also increase their resiliency against natural disasters, and it is also expected that the cost of network blackout is low in these conditions.
- Most research works exploit DRP and static energy storage devices such as batteries due to low time constants to improve the flexibility of the power system in the presence of RESs [16–19]. However, using a static storage device requires installation cost. But, EVs can also be used as a source of flexibility because they include battery. Since EVs and DRPs are owned by energy consumers and are distributed throughout the network, it is expected that no additional costs will be incurred to improve network flexibility under these conditions. This case has been investigated in few studies such as [20].
- The resiliency problem of distribution system and operation of VPPs is nonlinear programming (NLP) or mixed-integer NLP (MINLP). In some researches such as [27,28] to solve the mentioned problem, first, a linear approximation model is obtained for it and then the optimal solution is extracted using conventional solvers such as Simplex. Note that this case has a significant computational error compared to the original model of the problem so that the use of linearized AC power flow has a computational error above 10 % for power losses. Furthermore, some other researches such as [16,29,30] utilize non-hybrid evolutionary algorithms (NHEA) [16] and conventional mathematical solutions for NLP and MINLP problems [29,30] so that the optimal solution is obtained. However, because solvers lack unique response conditions, their response has low reliability.

1.4. Contributions

According to the above mentioned research gaps, the current study focuses on the operation of the SDN with FRVPPs constrained by network resiliency against flood and earthquake, as shown in Fig. 1. The FRVPP in the proposed design consists of RESs and flexibility sources such as EVs and DRPs. The suggested design attempts to minimizes the operating and shutting down costs associated with the SDN during floods and earthquakes. In this case, the shutdown cost is a function of expected energy not-supplied (EENS) due to natural disasters, which together with EENS are considered as resiliency indices in this paper. Constraints of the problem include AC power flow (AC-PF) equations, network operation and resiliency constraints, and the FRVPP operation model. It is worth noting that in this scheme, the load, energy price, RESs generation power, EVs energy demand, and availability of SDN equipment and FRVPP elements are uncertainties. Following this, the hybrid stochastic-robust programming (HSRP) is incorporated so that these uncertainties are appropriately modeled. The hybrid meta-heuristic algorithm (HMA)-based adaptive robust optimization ARO, i.e. HMA-based ARO, helps to accurately model the first four uncertainty

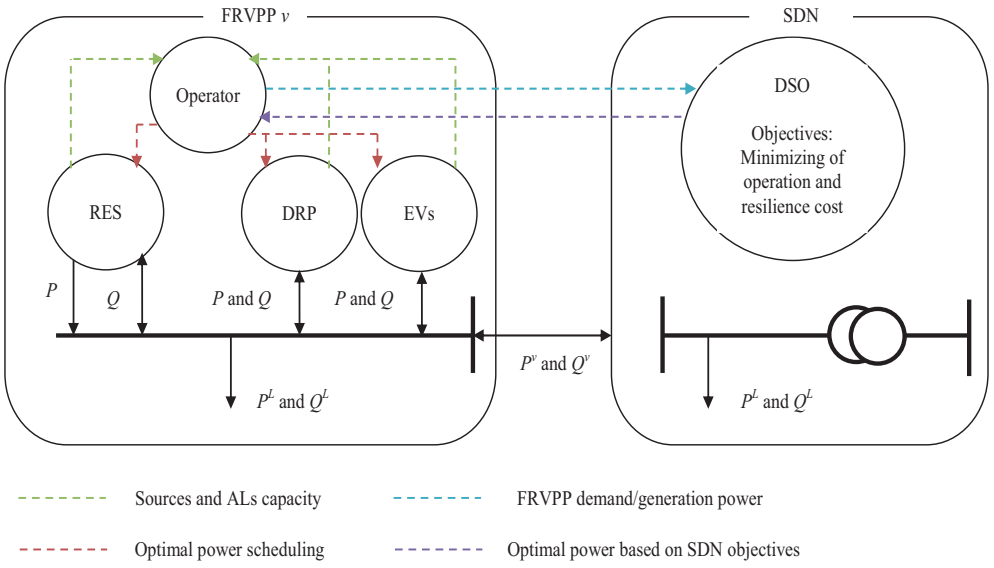

Fig. 1. The framework of the suggested design.

parameters. To provide a model for the last uncertainty, stochastic programming is adopted so that the Monte Carlo simulation (MCS) generates scenarios. Next, the simultaneous backward method (SBM) as a scenario reduction technique selects highly probable scenarios with short distance from each other. Since the exact number of resiliency indices is available in the case of analysis of several availability conditions of network equipment and FRVPP elements, stochastic programming was used for the last uncertainty. Robust modeling gives models of other uncertainty parameters and improves the solution time, and it will evaluate the FRVPP capability to enhance network resiliency in the worst-case scenario. The HMA based on the combination of krill herd optimization (KHO) and sine-cosine algorithm (SCA) is adopted to solve this problem to achieve the optimal solution and cover the third research gap. As this solver updates decision variables within different processes, it is predicted that the dispersion of the final response is low, which is corresponding to the unique response conditions. Finally, the contributions and objectives of the proposed design include:

- Resilient operation of an SDN with FRVPPs distributed throughout the network;
- Evaluation of the capability of FRVPPs in providing resiliency to the SDN during natural disasters, even for the worst-case scenario;
- Accurate calculation of resiliency indices by considering stochastic modeling of uncertainties of network equipment and FRVPP elements availability;
- Using HMA algorithm based on the combination of KHO and SCA to find the optimal solution with unique approximate response conditions; and
- Utilizing the HMA-based ARO technique for robust modeling of NLP and MINLP problems.

1.5. Paper origination

The layout of the paper is given here. Section 2 formulates the proposed problem is presented, then Section 3 describes the HSRP model. Section 4 addresses the HMA-based solution process. Results are presented in Section 5, and a summary of conclusions are reported in Section 6.

2. Problem formulation

The problem of an SDN with FRVPPs, resilient against flood and earthquake, is formulate in this section. This scheme attempts to minimize the total expected operating and shutdown costs to assess the operation state and optimal resiliency against the mentioned natural disasters. The constraints include AC optimal power flow (AC-OPF) equations, the network resiliency limit, and the operation model of FRVPP with RESs and FSs. Therefore, the model of the problem in the mentioned scheme is described as follows.

A) *Objective functions*: The objective function, Eq. (1), of the proposed scheme consists of two terms. The first term minimizes the expected cost of SDN energy purchase from the upstream network [31]. The second term minimizes the expected cost of system outage in the case of floods or earthquakes, which is considered in this article, as [27,28], as an index to evaluate the resiliency status of the SDN. This cost is calculated by multiplying the EENS and the value of lost load (VOLL). The objective function is commensurate with social welfare goals because, in the event of natural disasters, energy customers tend to minimize their interruption duration. Besides, they always seek to keep their energy costs to a minimum, whether or not natural disasters occur.

$$min \quad Cost = \sum_{\substack{t\in\Lambda_T \\ s\in\Lambda_S}} \pi_s \lambda_{t,s} P^{DS}_{ref,t,s} + VOLL. \overbrace{\sum_{\substack{n\in\Lambda_N \\ t\in\Lambda_T \\ s\in\Lambda_S}} \pi_s P^{NS}_{n,t,s}}^{EENS} \tag{1}$$

B) *SDN constraints*: Network constraints in the proposed problem include AC-PF equations, (2)-(7) [8], network operation constraints (8)-(10) [31], and system resiliency (11) [27]. The AC-PF constraints show active-reactive power balance at the network terminals, respectively, (2) and (3), the active and reactive power on distribution lines, (4) and (5), and the slack bus voltage angle and magnitude, (6) and (7), (8). Also, SDN operation constraints, such as (8)–(10), include constraints on the size of distribution line and substation and bus voltage range limits, respectively [31]. The equations assume that a distribution substation placed on the slack bus connects the SDN to the upstream network. Hence, for the slack bus, we have non-zero P^{DS} and Q^{DS}, while they are zero for the rest of buses [58]. Besides, in (10), the upper limit of the voltage range is used to prevent insulation damage to the equipment caused by overvoltage. Moreover, its low limit is to prevent consumers from interruption resulting from high voltage drop (8) [68]. Finally, the SDN resiliency limit is presented in (11), which indicates the switched-off load limit of individual buses [27].

$$P^{NS}_{n,t,s} + P^{DS}_{n,t,s} + \sum_{v\in\Lambda_{VPP}} A_{n,v}P^{V}_{v,t,s} - \sum_{j\in\Lambda_N} B_{n,j}P^{DL}_{n,j,t,s} = P^{L}_{n,t,s} \quad \forall n,t,s \tag{2}$$

$$Q^{DS}_{n,t,s} + \sum_{v\in\Lambda_{VPP}} A_{n,v}Q^{V}_{v,t,s} - \sum_{j\in\Lambda_N} B_{n,j}Q^{DL}_{n,j,t,s} = Q^{L}_{n,t,s} \quad \forall n,t,s \tag{3}$$

$$P^{DL}_{n,j,t,s} = g_{n,j}\left(V_{n,t,s}\right)^2 - V_{n,t,s}V_{j,t,s}\left\{g_{n,j}cos\left(\phi_{n,t,s}-\phi_{j,t,s}\right) + b_{n,j}sin\left(\phi_{n,t,s}-\phi_{j,t,s}\right)\right\}u^{DL}_{n,j,s} \quad \forall n,j,t,s \tag{4}$$

$$Q^{DL}_{n,j,t,s} = -b_{n,j}\left(V_{n,t,s}\right)^2 + V_{n,t,s}V_{j,t,s}\left\{b_{n,j}cos\left(\phi_{n,t,s}-\phi_{j,t,s}\right) - g_{n,j}sin\left(\phi_{n,t,s}-\phi_{j,t,s}\right)\right\}u^{DL}_{n,j,s} \quad \forall n,j,t,s \tag{5}$$

$$\phi_{n,t,s} = 0 \quad \forall n = \text{Slack bus}, t, s \tag{6}$$

$$V_{n,t,s} = V_{ref} \quad \forall n = \text{Slack bus}, t, s \tag{7}$$

$$\sqrt{\left(P^{DL}_{n,j,t,s}\right)^2 + \left(Q^{DL}_{n,j,t,s}\right)^2} \le \overline{S}^{DL}_{n,j} \quad \forall n,j,t,s \tag{8}$$

$$\sqrt{\left(P^{DS}_{n,t,s}\right)^2 + \left(Q^{DS}_{n,t,s}\right)^2} \le \overline{S}^{DS}_{n} u^{DS}_{n,s} \quad \forall n = \text{Slack bus}, t, s \tag{9}$$

$$\underline{V} \le V_{n,t,s} \le \overline{V} \quad \forall n,t,s \tag{10}$$

$$0 \le P^{NS}_{n,t,s} \le P^{L}_{n,t,s} \quad \forall n,t,s \tag{11}$$

C) *FRVPP constraints*: The FRVPP equations in the presence of RESs and flexibility sources (FSs), including DRP and EV parking lot, are expressed in (12)–(23). Constraints (12) and (13) describe active and reactive power balance in this system. In (14) and (15), the active power generated by photovoltaics (PVs) and wind turbines (WTs) is modeled. Then, the limit of apparent power flowing through these RESs is formulated in constraints (16) and (17) [57]. It is noteworthy that a DC/AC inverter connects PVs to the network [32]. WTs also have an asynchronous generator and an AC/AC converter connects WTs to the grid [32]. Therefore, by adopting a suitable structure for the mentioned converters (e.g. selecting the IGBT bridge for the converters) and the asynchronous generator, the converters will be capable of controlling reactive power [32]. Therefore, constraints (16) and (17) also consider the reactive power control capability of the RESs. Furthermore, constraints (18) and (19) express the operating model of the incentive-based DRP (IDRP) [20]. In this type of DRP, because energy cost is minimized in the objective function [66,67], customers reduce their energy consumption within peak period when energy price is high [61]. Then, during off-peak interval corresponding with low energy prices, customers are supplied with their reduced energy consumption during off-peak hours [62]. Hence, constraint (18) represents the limitation of DRP active power control, and constraint (19) ensures that customers participating in the IDRP reduce their consumed energy within inexpensive energy price period [20]. Finally, the constraints on the EVs parking lot are presented in (20)–(23) [31], which introduce the limits of charge and discharge rates of EVs, (20) and (21) [70], energy storage in their batteries, (22), and the charger capacity of EVs, (23) [69]. Parameter CR (DR / $\overline{S}^{EV}$) at time t equals the overall charge rate (discharge rate/charger capacity) of the EVs connected to the network for that time [31]. Also, the E^{Arr} (E^{Dep}) at any given time equals the sum of the arrival energy (energy required for travel) of the newly plugged-in (plugged-out) EVs to (from) the network at that period [60]. The arrival energy of an EV is calculated by multiplying its battery capacity (BC) and the state of charge (SOC), while energy required for travel is equal to BC, i.e., the full charge status is considered [31]. Additionally, the binary variable x represents the state of charge or discharge performance of EVs in the parking lot, so that $x = 1$ indicates the charging status, otherwise, it refers to the discharging status of EVs.

$$P^{V}_{v,t,s} = P^{PV}_{v,t,s} + P^{W}_{v,t,s} + \left(P^{DIS}_{v,t,s} - P^{CH}_{v,t,s}\right) + P^{DR}_{v,t,s} - P^{L}_{v,t,s} \quad \forall v,t,s \tag{12}$$

$$Q^{V}_{v,t,s} = Q^{PV}_{v,t,s} + Q^{W}_{v,t,s} + Q^{EV}_{v,t,s} - Q^{L}_{v,t,s} \quad \forall v,t,s \tag{13}$$

$$P^{PV}_{v,t,s} = \overline{P}^{PV}_{v,t,s} u^{PV}_{v,s} \quad \forall v,t,s \tag{14}$$

$$P^{W}_{v,t,s} = \overline{P}^{W}_{v,t,s} u^{W}_{v,s} \quad \forall v,t,s \tag{15}$$

$$\sqrt{\left(P^{PV}_{v,t,s}\right)^2 + \left(Q^{PV}_{v,t,s}\right)^2} \le \overline{S}^{PV}_{v} u^{PV}_{v,s} \quad \forall v,t,s \tag{16}$$

$$\sqrt{\left(P^{W}_{v,t,s}\right)^2 + \left(Q^{W}_{v,t,s}\right)^2} \le \overline{S}^{W}_{v} u^{W}_{v,s} \quad \forall v,t,s \tag{17}$$

$$-\gamma_v P^{L}_{v,t,s} \le P^{DR}_{v,t,s} \le \gamma_v P^{L}_{v,t,s} \quad \forall v,t,s \tag{18}$$

$$\sum_{t\in\Lambda_T} P^{DR}_{v,t,s} = 0 \quad \forall v,s \tag{19}$$

$$0 \le P^{CH}_{v,t,s} \le CR_{v,t,s}x_{v,t} \quad \forall v,t,s \tag{20}$$

$$0 \le P^{DIS}_{v,t,s} \le DR_{v,t,s}\left(1-x_{v,t}\right) \quad \forall v,t,s \tag{21}$$

$$\left(E^{Arr}_{v,t,s} - E^{Dep}_{v,t,s}\right)u^{EV}_{v,s} + \sum_{i=1}^{t}\left(\eta^{CH}P^{CH}_{v,i,s} - \frac{1}{\eta^{DIS}}P^{DIS}_{v,i,s}\right) \ge 0 \quad \forall v,t,s \tag{22}$$

$$\sqrt{\left(P^{DIS}_{v,t,s} - P^{CH}_{v,t,s}\right)^2 + \left(Q^{EV}_{v,t,s}\right)^2} \le \overline{S}^{EV}_{v,t,s} u^{EV}_{v,s} \quad \forall v,t,s \tag{23}$$

The model described by (1)–(23), the parameters u^{DL}, u^{DS}, u^{PV}, u^{W}, and u^{EV} represent the availability of distribution lines and substations, PV, WT, and EV parking lots in the case of floods and earthquakes. Thus, if u is equal to one for each of the mentioned elements, then that element is connected to the network in the mentioned conditions, otherwise, it is disconnected from the network.

3. Uncertainties modeling by the HSRP

The uncertainties associated with the problem, (1)–(23), include active and reactive load, P^L and Q^L, the maximum active power generation by WTs and PVs, $\overline{P}^W$ and $\overline{P}^{PV}$, energy price, λ, charge and discharge rates of EVs, CR and DR, arrival energy and departure energy of EVs, E^{Arr}

and E^{Dep}, the charging capacity of EVs, $\overline{S}^{EV}$ and the availability of network equipment and the FRVPP elements, u^{DL}, u^{DS}, u^{PV}, u^{W}, and u^{EV} are uncertainties. Since the number of uncertainty parameters is high, it is essential to extract many scenarios to achieve a guaranteed solution using stochastic and probabilistic programming [64,65], in which case problem-solving will be time-consuming. Therefore, the HSRP is incorporated in this study to model the uncertainties mentioned in the proposed scheme. In this design, the EENS index assesses the network resiliency. The exact value of this index based on [28] is available provided that different scenarios of equipment availability, such as u^{DL}, u^{DS}, u^{PV}, u^{W}, and u^{EV}, are taken into account. Therefore, stochastic modeling for these uncertainties is considered. Other uncertainties will also be based on robust modeling. This modeling requires a scenario known as the "*worst-case scenario*" [33]. This scenario also has some uncertainties that create the worst conditions for the problem, i.e., reduce the solution space of the problem. HSRP is therefore a convenient method for modeling uncertainties and has a lower computational time than stochastic and probabilistic programming [8]. Moreover, FRVPP will be a source of uncertainty due to the uncertainty in the behavior of RESs and EVs. It is also envisaged to be a good source to increase the resiliency of the distribution network. Hence, robust modeling of its uncertainties achieves the robust capability of the FRVPP to achieve a flexible network. In other words, in the event of a flood or earthquake, the answer to the question "*Is the FRVPP able to improve SDN resiliency in the worst-case scenario?*" is evaluated.

3.1. Stochastic programming

In the stochastic programming for uncertainties of availability of network equipment and FRVPP elements, the MCS first generates so many scenarios [59]. In each scenario, Bernoulli's probability distribution function (PDF) was adopted to find the probability values of parameters u^{DL}, u^{DS}, u^{PV}, u^{W}, and u^{EV} [27]. For instance, the probability of availability of WT (π^{W}) in a scenario will be proportional to $\pi^{W}_{v,s} = (1 - u^{W}_{v,s})FOR^{W}_{v}(1 - FOR^{W}_{v})\pi^{0}$ [27]. π^{0} indicates the probability of occurrence of a scenario in which no equipment or element is disconnected from the network and it can be calculated from [24].

$$\pi^{0}=\left(1-FOR^{DS}_{ref}\right)\prod_{(n,j)\in\Lambda_{N}}\left(1-FOR^{DL}_{n,j}\right)\prod_{v\in\Lambda_{VPP}}\left(1-FOR^{PV}_{v}\right)\left(1-FOR^{W}_{v}\right)\left(1-FOR^{EV}_{v}\right) \tag{24}$$

In this equation, FOR represents the forced outage rate (FOR) of network devices and FRVPP elements during floods and earthquakes. Note that, in the proposed scheme, the resistance of network elements against natural disasters is considered as an input parameter. This parameter is called Forced Outage Rate (FOR) for elements. If the FOR is low for an element, it means that element has low resilience against natural disasters. Therefore, the probability of the outage of the given element from the network is high. So, in the proposed scheme, for different natural disasters, there are different FORs for network equipment and FRVPP. In the following, the probability of outage of an element is based on the Bernoulli distribution, which is calculated based on Eq. (24). Furthermore, the occurrence probability for each scenario can be found by multiplying the probabilities of u^{DL}, u^{DS}, u^{PV}, u^{W}, and u^{EV}. The SBM is then employed to decrease the number of scenarios by selecting a specific number of scenarios generated by the MCS that are close to each other and have a high occurrence probability. For mor information about this method, the eager reader can refer to [34].

3.2. Robust programming

The current study employs the ARO to model the uncertainties of P^{L}, Q^{L}, λ,$\overline{P}^{W}$,$\overline{P}^{PV}$, CR, DR, E^{Arr}, E^{Dep}, and $\overline{S}^{EV}$. Since in this method only one scenario is needed for the mentioned parameters [33], the index s is removed from these uncertainty parameters. Thereby, the matrix of uncertainty parameters required by ARO ($\overline{u}$) is defined as [25]. According to this equation, the number of rows is equal to the number of operating hours (n_T), and the number of its columns (n_C) is equal to $n_C = 2n_B + 9n_V + 1$, where n_B is network buses number, and n_V denote FRVPPs number. True value for the mentioned uncertainties in ARO is variable, which is known as the uncertainty variable (u). Therefore, for the matrix $\overline{u}$, the matrix of uncertainty variables is presented as [26]. Then, based on [33], there is a need to define the uncertainties set for the ARO technique for these uncertainties, which is expressed for the t-th row of the matrix u as [27].

$$\overline{u} = \left[\lambda_{t}\, P^{L}_{t,n}\, Q^{L}_{t,n}\, P^{L}_{t,v}\, Q^{L}_{t,v}\, \overline{P}^{W}_{t,v}\, \overline{P}^{PV}_{t,v}\, CR_{t,v}\, DR_{t,v}\, E^{Arr}_{t,v}\, E^{Dep}_{t,v}\, \overline{S}^{EV}_{t,v}\right] \tag{25}$$

$$u = \left[\lambda^{u}_{t}\, P^{u}_{t,n}\, Q^{u}_{t,n}\, P^{u}_{t,v}\, Q^{u}_{t,v}\, \overline{P}^{uW}_{t,v}\, \overline{P}^{uPV}_{t,v}\, CR^{u}_{t,v}\, DR^{u}_{t,v}\, E^{uArr}_{t,v}\, E^{uDep}_{t,v}\, \overline{S}^{uEV}_{t,v}\right] \tag{26}$$

$$\Lambda^{u}_{t} = \left\{ u_{t} \in R^{n_C} : \frac{1}{n_C}\sum_{i=1}^{n_C}\frac{\left|u_{i,h} - \overline{u}_{i,t}\right|}{\widetilde{u}_{i,t}} \le \Delta\,,\ \forall u_{i,t} \in \left[\overline{u}_{i,t} - \widetilde{u}_{i,t}, \overline{u}_{i,t} + \widetilde{u}_{i,t}\right] \right\}\ \forall t \tag{27}$$

In (27), $\overline{u}$ has the predicted uncertainty value and $\widetilde{u}$ denotes the uncertainty deviation. Δ is the uncertainty budget within [0 1]. A zero indicates the deterministic state of uncertainty u, but if it is 1, it indicates that the state of all the elements of the matrix u is indeterministic (33). Moreover, the term $\left[\overline{u}_{i,t} - \widetilde{u}_{i,t}, \overline{u}_{i,t} + \widetilde{u}_{i,t}\right]$ represents the amplitude of change of an uncertainty matrix element. Finally, the set of uncertainties will be equal to unions of Λ^{u}_{t}as given in (28).

$$\Lambda^{u} = \underset{t\in\Lambda_{T}}{\cup}\Lambda^{u}_{t} \tag{28}$$

In the ARO technique, the worst-case scenario and the corresponding optimal point are determined at the same time [33]. In this technique, the objective function associated with the worst-case scenario has the worst value compared to other scenarios. For instance, should the objective function of the main problem to minimized, a higher value is obtained for the objective function in the worst-case scenario compared to other scenarios. To present the mathematical model of this topic, the term max is used in the uncertainty set in the objective function of the main problem, so that correct value of uncertainty variable (u) is determined. Hence, in this case, the variable u replaces the uncertainty parameter ($\overline{u}$). Also, the constraints of the robust problem based on ARO will be the same as the constraints of the main problem and (28) [33]. Therefore, for the problem (1)–(23), the ARO-based robust modeling is expressed as follows:

$$min_{y} max_{u\in\Lambda^{u}}\ \ Cost = \sum_{\substack{t\in\Lambda_{T}\\ s\in\Lambda_{S}}}\pi_{s}\lambda^{u}_{t}P^{DS}_{ref,t,s} + VOLL.\sum_{\substack{n\in\Lambda_{N}\\ t\in\Lambda_{T}\\ s\in\Lambda_{S}}}\pi_{s}P^{NS}_{n,t,s} \tag{29}$$

Subject to

Constraints (2) – (23) with replacing uncertainty parameters of (25) with uncertainty variables of matrix u and removing the index s (30)

Eq.(28) (31)

In problem (29)–(31), the variable y represents the vector of the variables of the problem (1)–(23) including the active and reactive power of different elements, the binary variable x, and the voltage magnitude and angle of the SDN buses. Term of min in (29) uses to obtain optimal value of y based on the original problem, (1)–(23), and term max in (25) achieves values of uncertainty parameters related to the worst-case scenario. Robust model constraints, (30), are same with Eqs. (2)–(23), but the variable u replaces to the parameter $\overline{u}$ (33). Constraint (31) is expressed limit of variable u (33). According to the problem (1)–(23), the binary variable x is independent of uncertainty and is known as the "*wait and see*" variable. Other variables of this problem depend on uncertainty, which is referred to as "*here and now*". Also, according to the problem (29)–(31), the variable u is independent of the uncertainty of availability of network equipment and FRVPP elements. Since the index s is removed from the variable u in problem (29)–(31), its independence from the uncertainty of the availability of SDN and FRVPP elements is observed. Yet, this does not observe the independence of the variable x from uncertainties. To solve this challenge, the term $min_x \sum_{\substack{t\in\Lambda_T \\ v\in\Lambda_{VPP}}} x_{v,t}$ is added as (32) to the objective function of the robust problem.

$$min_{x\in\{0,1\}}\left(\sum_{\substack{t\in\Lambda_T \\ v\in\Lambda_{VPP}}} x_{v,t}\right) + min_y max_{u\in\Lambda^u}\left(\sum_{\substack{t\in\Lambda_T \\ s\in\Lambda_S}} \pi_s \lambda_t^u P^{DS}_{ref,t,s} + VOLL.\sum_{\substack{n\in\Lambda_N \\ t\in\Lambda_T \\ s\in\Lambda_S}} \pi_s P^{NS}_{n,t,s}\right) \quad (32)$$

In (32), the value of x is determined according to the objective function $min_x \sum_{\substack{t\in\Lambda_T \\ v\in\Lambda_{VPP}}} x_{v,t}$ and the set {0, 1}, thereby its independence from uncertainties is observed. It should also be noted that according to the problem (1)–(23), the value of x is so determined that SDN shutdown cost plus operation costs is minimum. Since $x = 1$ indicates the state of charge of EVs and as EVs receive power from the network in this operating mode, the number of operating hours of EVs in the charging mode should be minimized to minimize the costs. This can be extracted in line with selecting $min_x \sum_{\substack{t\in\Lambda_T \\ v\in\Lambda_{VPP}}} x_{v,t}$. In other words, the first part of the objective function (32) is in line with the objective function (1).

4. HMA-based solution

4.1. Motivation to HMA using

The objective function (32) subject to constraints (30)–(31) is an MINLP problem. If one aims to solve the problem by using mathematical solvers, the dual model of the second part of (32) should be extracted until the *min-max* term becomes a *max* or *min* term. However, since finding the dual model of an MINLP problem requires observing duality gap and complementarity (equilibrium) constraints, the original formulation is difficult to obtain and will also complicate the solution process (35). To this end, in most researches such as (8), (33), a linear approximation formulation is first obtained for robust modeling of an optimization problem. However, this technique is associated with computational errors, and computational error for power losses in linear AC-OPF problem is higher than 10 % compared to that of the nonlinear model in the distribution network (8). Therefore, the solution obtained from this method has a small reliability coefficient. Another solution is to use evolutionary algorithms (EAs). In this method, a type of EA is generally exploited that can obtain a more optimal point. However, in NHEAs, dispersion of the final response has a significant value, which makes these algorithms lack unique response conditions. HMA can be used to address this issue. In this technique, decision variables are updated in several different processes, so it is expected that HMA can achieve a unique approximate response. To prove this, one can refer to the use of the mutation process in the genetic algorithm (GA) [36]. In this algorithm, using the mutation process, decision variables are updated in two processes (GA process and mutation). Finally, in this algorithm, a more optimal point with lower dispersion in the final response is obtained compared to that of the non-mutant GA [36]. Thus, the HMA based on a hybrid KHO [37]-SCA [38] algorithm is utilized in the present paper.

4.2. Solution method

In the proposed problem, the decision variables include P^{DIS}, P^{CH}, P^{DR}, P^{NS}, Q^{PV}, Q^{W}, Q^{EV}, x, and the uncertainty variable u. Therefore, EA and/or the mentioned algorithm, i.e., SCA + KHO, updates these variables based on constraints (21), (20), (18), (11), intervals $[0, \overline{S}^{PV}u^{PV}]$, $[0, \overline{S}^{W}u^{W}]$, $[0, \overline{S}^{EV}u^{EV}]$, sets {0, 1} and Λ^u, respectively. Then, the dependent variables of P^{DS}, P^{V}, P^{DL}, P^{PV}, P^{W}, Q^{DS}, Q^{V}, Q^{DL}, V, and ϕ can be found observing constraints (2)–(7) and (12)–(15) and decision variables. To put is simply, initially, the values of variables P^{V}, P^{PV}, P^{W}, and Q^{V} are determined using (12)–(15). Next, the values of other dependent variables are calculated based on the power flow Eqs. (2)–(7). The backward-forward method solves the power flow equations given in this study [39]. To estimate SDN operation limits, (8)–(10), capacity limit of RESs, (16)–(17), DRP constraint, (19), energy limit and EV charger capacity, (22)–(23), the penalty function method [40] is used. The penalty function for limit of $a \le b$ is equal to $\alpha.\max(0, a - b)$, and it for constraint of $a = b$ is as $\beta.(b - a)$. $\alpha \ge 0$ and $\beta \in (-\infty, +\infty)$ are Lagrangian multipliers that are considered as decision variables and are updated by SCA + KHO. In the next step, the fitness function (FF) is formed by adding the objective functions of the main problem (32) to all penalty functions. Note that constraints (8)–(10), (16)–(17), (19), and (22)–(23) depend on the uncertainty variables, so the penalty functions are added to the second part of (32). The value of FF is then found based on decision-making and dependent variables. Then, the optimal value is calculated and then the decision variables are updated according to the optimal value of the FF in the next steps. It is noteworthy that these steps continue until the convergence point is achieved. The convergence point is obtained after performing the maximum number of iteration (I_{max}) of updating the decision variables and Lagrange multipliers. Solution procedure steps using the SCA + KHO method are provided as follows:

- **Step1**: Generate N (population size) random values for decision variables and Lagrange multipliers considering their constraints.
- **Step 2**: Calculate the values of dependent variables and the fitness function for total population of decision variables and Lagrange multipliers, and then determine the optimal value of FF.
- **Step 3**: If the problem has converged, the procedure will be terminated, otherwise Step 4 will be performed. In this part, it is assumed that the convergence of the problem is achieved after updating the decision variables and Lagrange multipliers for I_{max} times.
- **Step 4**: Update the decision variables and Lagrange multipliers based on the optimal value of FF in the previous step, so that first SCA performs the updating and then KHO executes this process. Then, run Step 2.

5. Simulation results

5.1. Case studies

The problem is applied to the IEEE 69-bus SDN as illustrated in Fig. 2, where the specifications of the line and distribution substation and peak

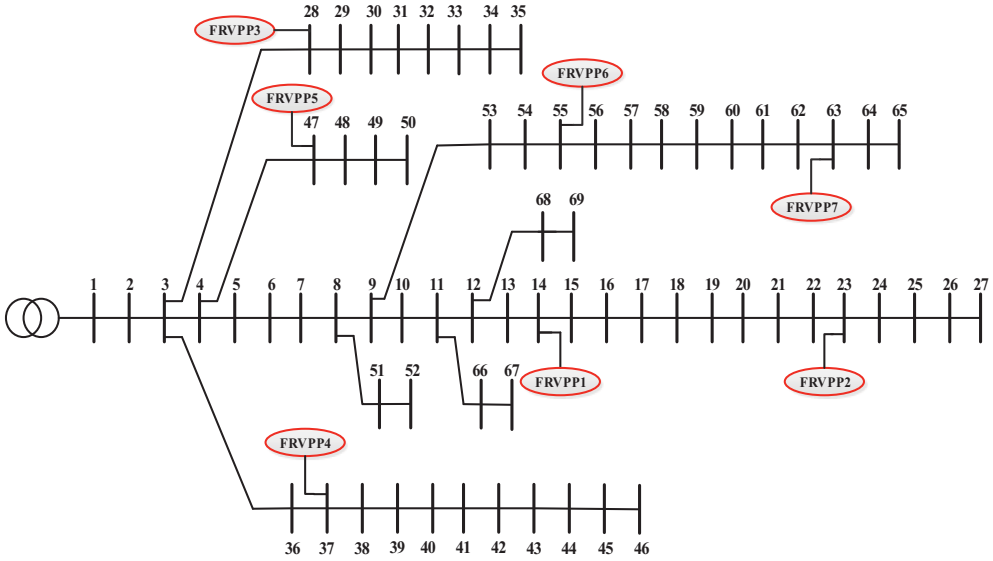

Fig. 2. The proposed test system [20].

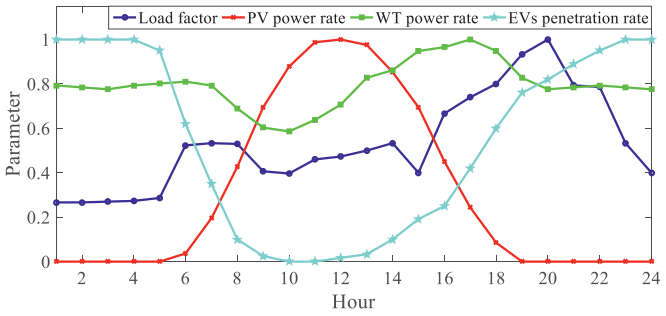

Fig. 3. Daily curve of load factor [20], RES power rate [20] and EVs penetration rate [51].

load data were extracted from (20). The base power and voltage are 1 MVA and 12.66 kV, and the permissible voltage range is [0.9, 1.05] p.u [41], [42], [43], [44], [45]. The daily load data is calculated by multiplying the peak load and the daily load factor curve, as shown in Fig. 3 [20]. Energy prices for 1:00–7:00, 8:00–16:00, and 23:00–00:00, and 17:00–22:00 are 16 $/MWh, 24 $/MWh, and 30 $/MWh, respectively [35]. The network has seven FRVPPs whose locations are shown in Fig. 2. FRVPPs 1, 2, 6, and 7 (3–5) are equipped with PV and WT units with capacity of 0.3 (0.5) MVA, and these FRVPPs include 150 (200) EVs [20]. The customer participation rate for these FRVPPs is also set at 50 % in the DRP, with peak data reported in [20]. Also, the daily power output profile of RESs, which are PV and WT, is the multiplication of its capacity and the daily power rate curve of RESs [46–50], as depicted in Fig. 3 [20]. Also, the daily profile of the number of EVs in FRVPP is proportional to the product of the total number of EVs and their penetration rate curve, which is depicted in Fig. 3 [51]. Other specifications of EVs including charge/discharge rate, SOC, battery capacity, charger capacity, and more are reported in [31,35,51]. It is assumed that floods may occur in areas including feeders between buses 1–27, 51–52, 66–67, and 68–69 in Fig. 2, and earthquakes may occur in other feeders, where the FOR of distribution lines is set 1 % against these natural disasters, and the distribution substation is set 10 %. This value is set at 10 % for FRVPP elements. MCS then generates 1000 scenarios for the uncertainty of availability of SDN equipment and FRVPP elements, which SBM then selects 60 generated scenarios. Concerning the robust model, the uncertainty deviation ($\widetilde{u}$) is calculated by multiplying the uncertainty level (r) and the uncertainty budget (Δ), where this uncertainty level for all uncertainties of the load, energy price, generation capacity of the RESs, and EV energy demand are considered the same. Finally, the VOLL is set at 100 $/MWh so that high resiliency is achieved for the SDN.

6. Results

The problem and the solution process mentioned in this paper are implemented using the MATLAB software. The obtained results are provided below.

A) *Evaluation of the HMA solver capability for the proposed problem*: In this part, SCA + KHO, KHO, SCA, Teaching and Learning-based Optimization (TLBO) [52], and Differential Eqs. (DE) [53] algorithms are incorporated so that the optimal solution is found. The details of these algorithms along with the necessary formulations are presented in [37,38,52,53]. In all these algorithms, it is necessary to determine the size of the population and the maximum iteration of convergence. SCA and TLBO algorithms do not have other setting parameters. In the DE algorithm, there are two other setting parameters, such as crossover rate and weighting rate, whose values were chosen as 0.8 and 0.3,

Table 2
Convergence results of the proposed problem obtained by different solvers for different values of the uncertainty level and $\Delta = 1$.

r	0				0.1			
Algorithm	Cost ($)	CI	CT (s)	SD (%)	Cost ($)	CI	CT (s)	SD (%)
SCA + KHO	1507.2	729	131.4	0.933	1648.3	786	136.2	0.934
KHO	1545.1	907	142.3	1.12	1689.1	997	149.1	1.19
SCA	1559.7	934	144.7	1.43	1705.5	1036	152.4	1.55
TLBO	1611.5	1226	162.5	2.05	1765.2	1331	172.8	2.34
DE	1638.3	1451	183.1	2.67	1796.8	1568	194.6	2.98

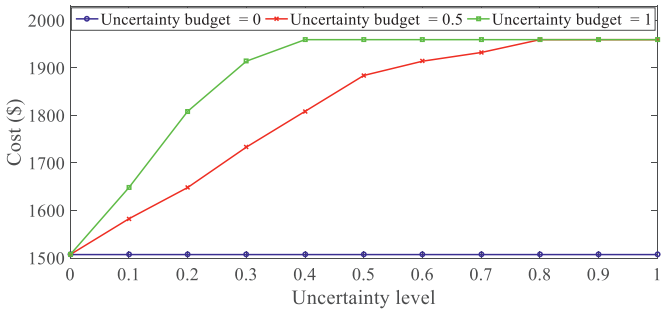

Fig. 4. Objective function curve for uncertainty level for different values of uncertainty budget.

respectively [53]. Other setting parameters in the KHO algorithm include mutation rate, crossover rate, position constant number, inertia weight of the foraging motion, and inertia weight of the motion induced, which are set at 0.15, 0.8, 1.5, 0.8, and 0.8, respectively [37]. The population size (N) and I_{max} for these solvers are 50 and 2000, respectively. To calculate the statistical indices of the problem response such as standard deviation (SD), the problem is solved using these algorithms 20 times. Table 2 reports the results, where the SCA + KHO algorithm finds the minimum value of the objective function or Cost function, that is $1507 (1648.3) at the convergence iteration (CI) number of 729 (786) for the HSRP model with zero uncertainty level (0.1). This algorithm obtains the mentioned convergence point in the computational time (CT) of 131.4 (136.2) s. Yet, other NHEA-based algorithms have a higher cost rate than SCA + KHO. Besides, they obtain the convergence point at a CI over 900 s and CT over 142 s for the proposed HSRP model for different levels of uncertainty. Alternatively, the SCA + KHO solver has an SD of about 0.93 %, while this parameter value for other algorithms is higher than 1.1 %. This means that the final response obtained by the algorithm is less dispersed than NHEAs. Hence, it has almost unique response conditions. Also, with changing the uncertainty level, the SD for the final response obtained by this algorithm changes slightly, but this is not the case for NHEAs. In other words, the dependence of the dispersion of problem solution by SCA + KHO on the volume of the problem is very small, so it can be inferred that by implementing the proposed problem on different data, it will always find the optimal solution with high reliability.

B) *Analysis of the suggested HSRB model*: Fig. 4 depicts the diagram of total expected operating and resiliency costs (Cost) of the SDN in terms of load uncertainty level, energy price, active power generation by RESs, and EV energy demand, i.e., r, in terms of different uncertainty budget (Δ) values associated with these parameters. According to this figure, for $\Delta = 0$ and $r = 0$, the Cost function is always constant and equal to $1507.2. Because in these circumstances, according to (27), the rate of deviation of these uncertainties is zero, so the true values of these uncertainties are always equal to their predicted values. Hence, the objective function value is fixed. Nonetheless, with increasing Δ, the Cost vs r curve is saturated so that for $\Delta = 0.5$ (1), the Cost function value remains always constant for changes in the uncertainty level at $r \geq 0.8$ (0.4). Also, for $r \leq 0.8$ (0.4), increasing the uncertainty level of the mentioned parameters increases the operating cost and resiliency of the SDN. The reason is that increasing r and Δ will increase the load, energy price, and energy consumption of EVs in the worst-case scenario compared to their predicted values (refer to Table 4). Nevertheless, under these conditions, the active power generation by RESs, charge/discharge rate, and charger capacity of EVs decrease in this scenario. Therefore, in general, it can be said that increasing the uncertainty level of the load, energy price, active power generation by RESs, and energy demand of EVs to achieve the worst conditions or a robust situation with respect to these uncertainties increases the energy consumption of active and passive loads., reduces the capacity of power generation sources, and increase the energy prices in the worst-case scenario. Consequently, operating and resiliency costs of the SDN increase with increasing r relative to the case with $r = 0$. Because according to (1), in order to minimize operating and resiliency costs, local sources and ALs must provide high power injection into the network, which in case of increasing r, their power injection based on Table 3 is reduced. Note, however, that excessive values of these uncertainties may make the problem infeasible. Thus, the ARO technique does not allow an excessive increase of these parameters based on (27), so for $r \geq 0.8$ (0.4) at $\Delta = 0.5$ (1), the Cost function always has a constant value.

C) *Investigation of FRVPPs performance*: Figs. 5 and 6 indicate the active and reactive power curves of FRVPPs and their elements for different values of uncertainty level and uncertainty budget 1. Referring to Fig. 5(a), the RESs inject high reactive power into FRVPPs between 7:00 and 18:00 because during these hours, according to Fig. 3, both types of RESs, namely PV and WT, produce active power. At other operating hours, only the WTs generate energy and the PVs are switched off (Fig. 3). Therefore, active power generation by all RESs during these hours is less than that of the period 7:00–18:00. Also, increasing the uncertainty level in all operating hours reduces the active power of RESs in comparison to a case with $r = 0$, confirming the results reported in Table 3. In the following, as illustrated in Fig. 5(b), customers participating in the proposed DRP increase energy consumption during the off-peak hours, 1:00–7:00, and mid-peak period 8:00–16:00 and 23:00–00:00 so that the percentage of increase during off-peak hours is higher than that of the mid-peak hours. However, they also consume less energy during peak

Table 3
Value of uncertainty parameters related to robust model for different values of uncertainty level and budget.

Δ	0			0.5			1		
r	0	0.1	0.2	0	0.1	0.2	0	0.1	0.2
Sum of λ^u ($/MWh)	556	556	556	556	583.8	611.6	556	611.6	667.2
Sum of P^u (p.u)	70.248	70.248	70.248	70.248	73.760	77.273	70.248	77.273	84.297
Sum of Q^u (p.u)	49.451	49.451	49.451	49.451	51.923	54.396	49.451	54.396	59.341
Sum of $\overline{P}^{uPV}$ (p.u)	20.316	20.316	20.316	20.316	19.300	18.284	20.316	18.284	16.253
Sum of $\overline{P}^{uW}$ (p.u)	51.487	51.487	51.487	51.487	48.912	46.338	51.487	46.338	41.189
Sum of CR^u (p.u)	49.869	49.869	49.869	49.869	47.375	44.882	49.869	44.882	39.895
Sum of DR^u (p.u)	49.869	49.869	49.869	49.869	47.375	44.882	49.869	44.882	39.895
Sum of E^{uArr} (p.u)	2.88	2.88	2.88	2.88	2.736	2.592	2.88	2.592	2.304
Sum of E^{uDep} (p.u)	14.4	14.4	14.4	14.4	15.12	15.84	14.4	15.84	17.28
Sum of $\overline{S}^{uEV}$ (p.u)	76.466	76.466	76.466	76.466	72.643	68.819	76.466	68.819	61.173

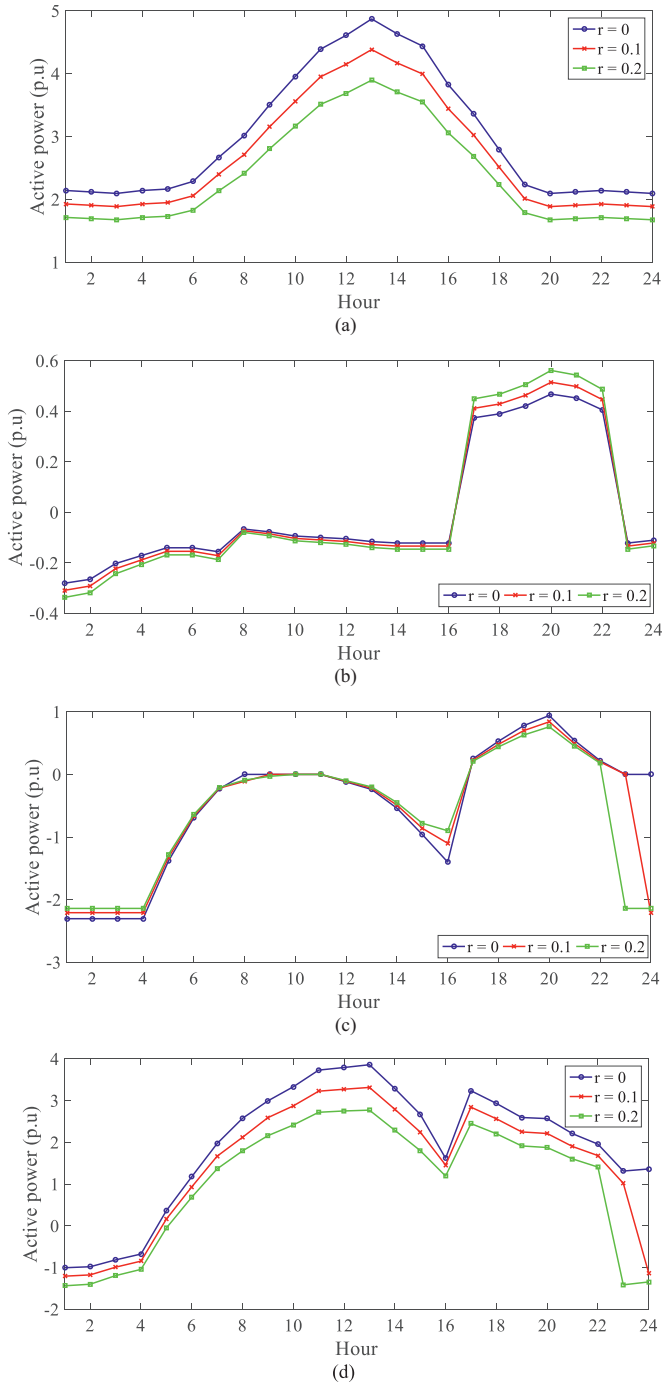

Fig. 5. Daily active power curve of, a) RESs, b) DRPs, c) EVs, d) FRVPPs for different values of uncertainty level and $\Delta = 1$.

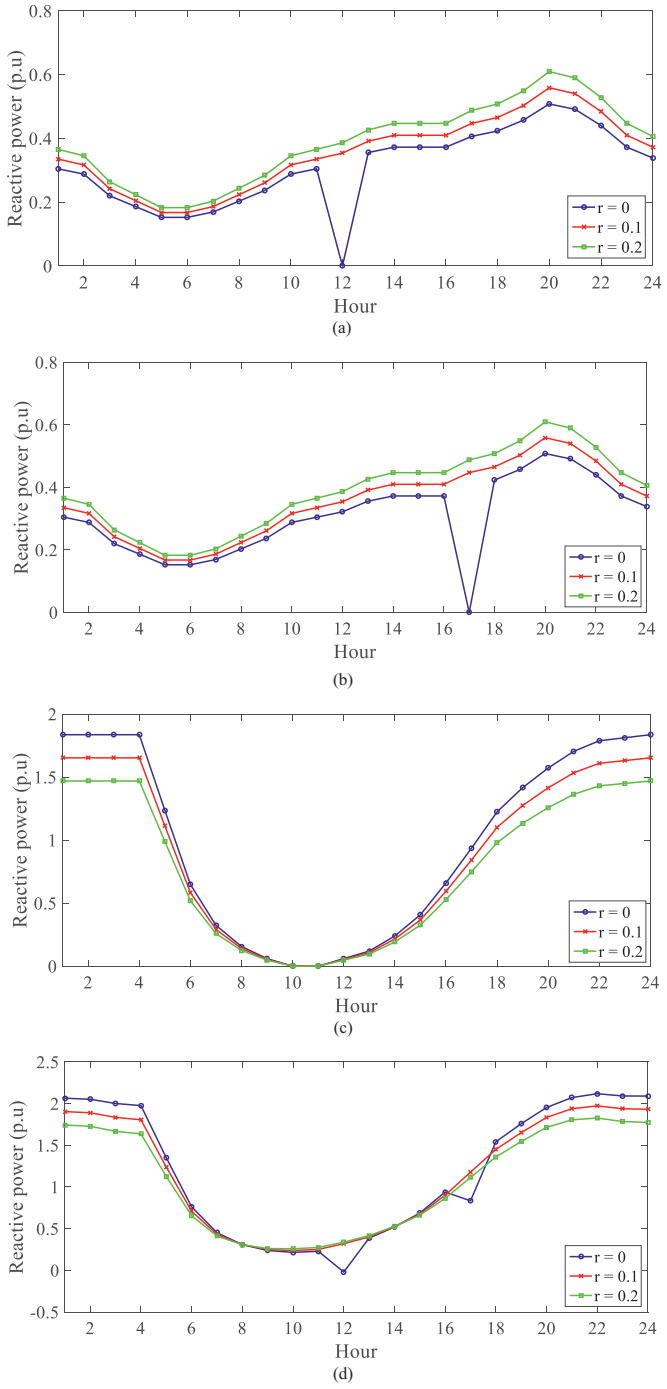

Fig. 6. Daily reactive power curve of, a) PVs, b) WTs, c) EVs, d) FRVPPs for different values of uncertainty level and $\Delta = 1$.

period. Such a performance relies on load data and energy prices and aims to minimize operating and resiliency costs so that during low energy price and load, customers consume more energy, and during the peak-period with high energy prices, they consume less energy. Also, according to (18), the performance of DRPs depends on the demand value. Therefore, in the worst-case scenario, a larger r increases the load compared to $r = 0$ according to Table 3. As a result, in these conditions, DRP power will increase both in the mode of decreasing consumption and in the mode of increasing consumption. This is also evident in Fig. 5(b). Fig. 5(c) shows the daily active power curve of EVs. As per Fig. 5 (c), EVs receive active power from FRVPP to supply their travel energy during off-peak hours. They also receive energy from the FRVPP from 12:00 to 16:00 so that they can inject this energy into the network during peak hours, 17:00–22:00. Because according to Section 4.1, energy prices are low in the off-peak period and 12:00–16:00 but are high in the off-peak period. Consequently, to reduce the operating cost, it is recommended to charge (discharge) EVs at inexpensive energy price periods. Furthermore, as shown in Fig. 5(c), increasing r decreases the charge and discharge power levels of EVs to the case $r = 0$, but their charging interval to supply EV travel energy increases compared to the previous case. The increase in the mentioned interval according to Table 3 is due to the increase in consumption of energy

required for EVs travel ($E^{Dep} - E^{Arr}$) in the mentioned conditions. Eventually, the daily active power curve of FRVPPs is proportional to Fig. 5(d), which is calculated from (12). According to this figure, FRVPPs with proper management of sources and ALs can inject active power into the SDN during most operating hours, 5:00–22:00, and act as a local source. This helps some network customers to be supplied by FRVPPs in the event of a flood or earthquake in the network or when some SDN equipment is disconnected, which confirms the ability of FRVPPs to enhance SDN resiliency. At 1:00–4:00 and 23:00–00:00 periods, the energy consumption by EVs and DRPs is higher than the energy generated by RESs, so during these hours, FRVPPs act as consumers.

Fig. 6 shows the daily reactive power curve of FRVPPs and their elements. As given in Eq. (13), reactive power sources of FRVPPs include RESs and EVs. According to Fig. 6(a)-(b), RESs generally provide a percentage of the network's reactive load at all hours of operation, so their daily reactive power curve is similar to the daily load factor curve. However, in hours when their active power output is high, such as 12:00 for PVs and 17:00 for WTs, the capacity of RESs to generate reactive power decreases. This is evident at 12:00 for Fig. 6(a) and at 17:00 for Fig. 6(b) at $r = 0$. Furthermore, increased uncertainty level in the worst-case scenario escalated reactive power generation by RESs compared to the case with $r = 0$ because according to Fig. 5(a), the active power of RESs decreases in these conditions and they can produce higher reactive power in these conditions based on (16) and (17). Fig. 6(c) shows the daily reactive power curve of EVs in FRVPPs. Based on this figure and Fig. 3, it can be stated that the amount of reactive power of EVs in FRVPP relies on the number of EVs, so that during the hours when the number of EVs is high (low), their injected reactive power is also high (low). Also, increasing r reduces EVs reactive power in all operating hours compared to $r = 0$. This is due to the reduction in EVs charger capacity in the worst-case scenario (Table 3). Eventually, the daily reactive power curve of FRVPPs based on (13) will be as shown in Fig. 6(d). Since the reactive power produced by EVs is higher than that of RESs, the impactability of EVs in controlling the reactive power of FRVPPs is greater than RESs. Hence, the daily reactive power curve of FRVPPs has a trend of changes similar to the curve in Fig. 6(c). Following this, increasing r reduces the reactive power of FRVPPs compared to $r = 0$.

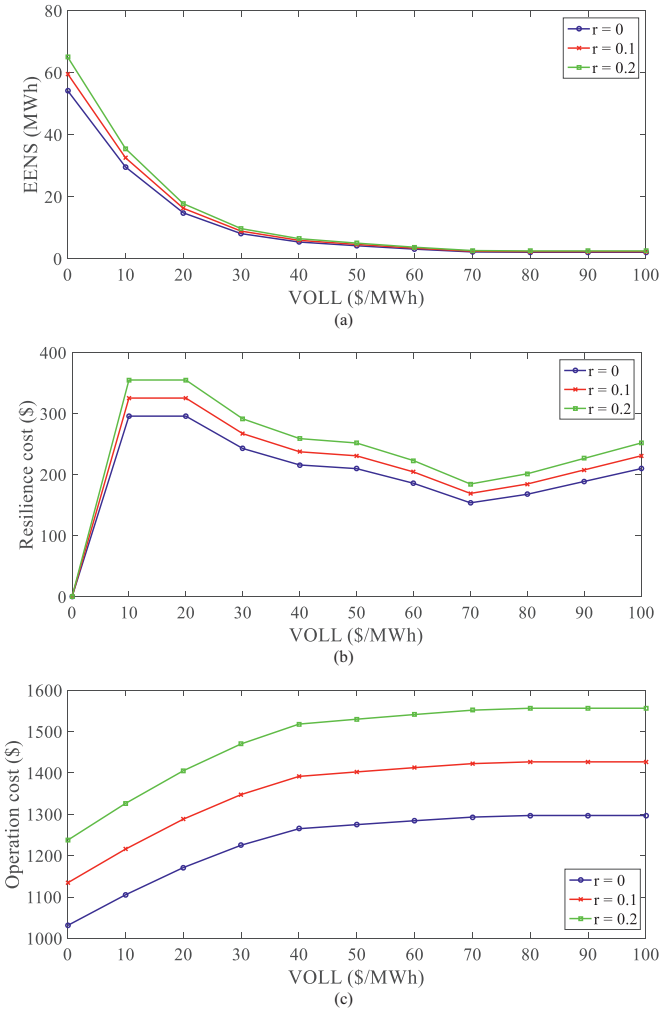

Fig. 7. Resiliency and economic indices curve, a) EENS, b) resilience cost, c) operation cost in VOLL for different values of uncertainty level and $\Delta = 1$.

D) *Evaluation of SDN technical indices*: Fig. 7 depicts the curve of resiliency indices, that are EENS and resiliency cost (the second part of (1)), and economic index, i.e., the operating cost (first part of (1)) in terms of VOLL for different values of uncertainty level and uncertainty budget 1. Fig. 7(a) shows that increasing the penalty price of the VOLL reduces the EENS in the SDN, so that for a VOLL greater than 70 $/MWh, the minimum value of the EENS is obtained for different values of r. Therefore, for the proposed scheme, following the data in Section 4.1, the penalty price to reduce the rate of blackouts caused by floods and earthquakes is 70 $/MWh. The diagram of the resiliency cost in terms of VOLL is shown in Fig. 7(b). The resiliency cost given in Eq. (1) is calculated by multiplying the EENS and VOLL. For VOLL values between 0 and 10 $/MWh, the increase in VOLL is greater than the decrease in EENS, so the resiliency cost increases in proportion to the increase in VOLL. Nonetheless, for VOLLs between 10 $/MWh and 70 $/MWh, the impact of decreasing EENS is greater than that of increasing VOLL. Hence, in this case, the resiliency cost decreases in proportion to the increase in VOLL.

At VOLL above 70 $/MWh, the EENS is fixed, and changes in the resiliency cost will only depend on changes in VOLL. In general, increasing the VOLL improves the SDN resiliency, but this increases the operating cost as well according to Fig. 7(c). Because in these conditions, supplying energy from the upstream network, which sells energy at a price of λ, is more economical and will be commensurate with the cost function minimization. Besides, energy supply by FRVPPs is also cost-effective during natural disasters, as RESs in FRVPPs have zero operating costs, and the performance of DRPs and EVs, as shown in Fig. 5, is such that the cost of energy purchased from the upstream network becomes minimum. Yet, since increasing VOLL increases the importance of minimizing the resiliency cost in (1) with respect to the operating cost of SDNs, EVs and DRPs attempt to inject high energy into the network. This also requires them to receive high energy during off-peak hours, which will be commensurate with the increase in operating costs compared to low VOLL cases. Besides, the increase in r due to the increase in energy consumption of FRVPPs and SDNs, the decrease in energy generation by FRVPPs, and the increase in energy prices according to Table 3 will increase EENS, and resiliency and operating costs, which is clear in Fig. 7.

Table 4
Technical indices value for different values of uncertainty level and $\Delta = 1$.

Case	I			II		
R	0	0.1	0.2	0	0.1	0.2
EENS (MWh)	42.1	46.3	50.5	2.11	2.28	2.45
EEL (MWh)	2.31	2.54	2.77	1.58	1.71	1.84
MVD (p.u)	0.091	0.094	0.097	0.0531	0.0548	0.0563
MOV (p.u)	0	0	0	0.0112	0.0108	0.0105

In the proposed scheme, EENS and outage cost (the second part of Eq. (1)) are included as resilience indicators. So, if the amount of these indicators is low, then social welfare is high in the event of natural disasters because the shutdown of consumers will be low. Therefore, in this situation, it can be said that the resilience of the network against natural disasters is high. Now, in order for the outage of consumers to be low in the conditions of natural disasters, it is necessary that in those conditions, resources, or substations or distribution lines are available. In the proposed scheme, based on Section 5.1, it is assumed that the resistance of FRVPPs against natural disasters is high, and since they are located in the consumption areas at the distribution network level, according to Fig. 2, if natural disasters occur and some of the network equipment like distribution lines are interrupted, FRVPPs are able to supply a portion of the energy consumption. Thus, they can obtain acceptable resilience in the network.

Eventually, SDN technical indicators [54,55,56] such as EENS, energy loss (EL), maximum voltage drop (MVD), and maximum overvoltage (MOV) for power flow analysis (I) and the suggested design (II) are analyzed and the results are listed in Table 4 for different values of uncertainty levels and uncertainty budget 1. As per Table 4, the design reduces EENS, EL, and MVD relative to the power flow so that in the worst-case scenario ($r = 0.2$), these parameters in the proposed scheme are approximately 95.15 % ((50.5–2.45)/50.5), 33.6 %, and 42 %, respectively, which are reduced in comparison to power flow studies. However, the decrease in MVD requires an increase in MOV of about 0.0105 p.u. in the mentioned conditions, which is smaller than the allowable limit of 0.05 (1.05–1) p.u. Therefore, it can be said that proper energy management of FRVPPs can enhance the resiliency and operation indices by roughly 95 % and 38 %, respectively.

7. Conclusion

This paper describes the operation of SDN with FRVPPs subject to network resiliency against flood and earthquake. FRVPPs utilized DRPs and EVs in the presence of RESs to establish flexibility. Subsequently, the proposed scheme minimized the total operating and resiliency costs of the SDN, where it was constrained by the optimal AC power flow equations, SDN resiliency against floods and earthquakes, and the operating model of FRVPPs. Then, the hybrid stochastic-robust planning (HSRP) was used to model the uncertainties, in which the stochastic planning part models the uncertainties associated with availability of SDN devices and FRVPP elements, and the robust planning based on the HMA-based ARO technique models the uncertainties associated with load, energy prices, active power generation by RESs, and EV energy demand. In this paper, HMA based on the hybrid SCA-KHO algorithm obtains the optimal solution. Referring to the results, the hybrid algorithm finds the optimal solution within minimum possible convergence iterations and computational time in comparison to NHEAs. Additionally, the SD of its final response to the proposed problem is around 0.93 %, which due to the low dispersion of its response has approximately unique response conditions. Additionally, in the worst-case scenario, the resulting uncertainties related to the robust model, the energy consumption of SDNs and FRVPPs, the energy generation capacity of the FRVPPs, and the energy price relative to the scenario with the predicted values of these uncertainties increased. However, with proper management of FRVPPs in the SDN under the proposed scheme, FRVPPs were able to improve the resiliency of the network against the flood and earthquake by roughly 95 % in comparison with power flow studies, even in the worst-case scenario. It also enhances network operation indicators like energy loss and voltage profile by approximately 33.6 % and 42 %, respectively, in comparison with power flow under these conditions.

CRediT authorship contribution statement

Ghasem Piltan Conceptualization, Methodology, Software, Validation, Writing- Reviewing and Editing, Data curation, Writing- Original draft preparation.

Sasan Pirouzi Conceptualization, Methodology, Software, Validation, Writing- Reviewing and Editing, Data curation, Writing- Original draft preparation.

Alireza Azarhooshang Conceptualization, Methodology, Software, Validation, Writing- Reviewing and Editing, Data curation, Writing- Original draft preparation.

Ahmad Rezaee Jordehi Validation, Writing- Reviewing and Editing, Data curation, Writing- Original draft preparation, Supervision.

Ali Paeizi Original draft preparation, Visualization, Reviewing and Editing, Discussion, Software

Mojtaba Ghadamyari Original draft preparation, Visualization, Reviewing and Editing

Declaration of competing interest

The authors declare that they have no known competing financial interests or personal relationships that could have appeared to influence the work reported in this paper.

Data availability

Data will be made available on request.

References

[1] M.R. AkbaïZadeh, T. Niknam, A. Kavousi-Fard, Adaptive robust optimization for the energy management of the grid-connected energy hubs based on hybrid metaheuristic algorithm, Energy 235 (2021) 121171.
[2] D. Wang, J. Qiu, L. Reedman, K. Meng, L. Lei Lai, Two-stage energy management for networked microgrids with high renewable penetration, Appl. Energy 226 (2018) 39–48.
[3] N. Rezaei, Y. Pezhmani, Optimal islanding operation of hydrogen integrated multi-microgrids considering uncertainty and unexpected outages, J. Energy Storage 49 (2022), 104142.
[4] M.H. Nozari, M. Yaghoubi, K. Jafarpur, G.A. Mansoori, Development of dynamic energy storage hub concept: a comprehensive literature review of multi storage systems, J. Energy Storage 48 (2022), 103972.
[5] A.R. Jordehi, V.S. Tabar, S. Mansouri, M. Nasir, S. Hakimi, S. Pirouzi, A risk-averse two-stage stochastic model for planning retailers including self-generation and storage system, J. Energy Storage 51 (2022), 104380.
[6] A.R. Jordehi, Two-stage stochastic programming for risk-aware scheduling of energy hubs participating in day-ahead and real-time electricity markets, Sustain. Cities Soc. 31 (2022), 103823.
[7] A.R. Jordehi, V.S. Tabar, S. Mansouri, F. Sheidaei, A. Ahmarinejad, S. Pirouzi, Two-stage stochastic programming for scheduling microgrids with high wind penetration including fast demand response providers and fast-start generators, Sustain. Energy Grid Netw. 30 (2022), 100694.
[8] S.A. Bozorgavari, J. Aghaei, S. Pirouzi, A. Nikoobakht, H. Farahmand, M. Korpås, Robust planning of distributed battery energy storage systems in flexible smart distribution networks: a comprehensive study, Renew. Sust. Energ. Rev. 123 (2020), 109739.
[9] A. Jamali, et al., Self-Scheduling approach to coordinating wind power producers with energy storage and demand response, IEEE Trans. Sustainable Energy 11 (2020) 1210–1219.
[10] S.A. Shirmardi, M. Joorabian, H. Barati, Flexible-reliable operation of green microgrids including sources and energy storage-based active loads considering ANFIS-based data forecastingmethod, Electr. Power Syst. Res. 210 (2022), 108107.
[11] A.R. Jordehi, Risk-aware two-stage stochastic programming for electricity procurement of a large consumer with storage system and demand response, J. Energy Storage 25 (2022), 104478.
[12] S. Ma, L. Su, Z. Wang, F. Qiu, G. Guo, Resilience enhancement of distribution grids against extreme weather events, IEEE Trans. Power Syst. 33 (2018) 4842–4853.
[13] W. Wang, P. Chen, D. Zeng, J. Liu, Electric vehicle fleet integration in a virtual power plant with large-scale wind power, IEEE Trans. Ind. Appl. 56 (2020) 5924–5931.

[14] Z.Z. Wu, et al., Optimal placement and sizing of the virtual power plant constrained to flexible-renewable energy proving in the smart distribution network, Sustainable Energy Technol. Assess. 49 (2022), 101688.
[15] A.Z.G. Seyyedi, et al., Bi-level sitting and sizing of flexi-renewable virtual power plants in the active distribution networks, Int. J. Electr. Power Energy Syst. 111 (2022), 104311.
[16] N. Lou, et al., Two-stage congestion management considering virtual power plant with cascade hydro-photovoltaic-pumped storage hybrid generation, IEEE Access 8 (2020) 186335–186347.
[17] A. Baringo, L. Baringo, J.M. Arroyo, Day-ahead self-scheduling of a virtual power plant in energy and reserve electricity markets under uncertainty, IEEE Trans. Power Syst. 34 (2019) 1881–1894.
[18] Z. Yi, Y. Xu, J. Zhou, W. Wu, H. Sun, Bi-level programming for optimal operation of an active distribution network with multiple virtual power plants, IEEE Trans. Sustainable Energy 11 (2020) 2855–2869.
[19] M. Rahimi, F. Jahanbani-Ardakani, A. Jahanbani-Ardakani, Optimal stochastic scheduling of electrical and thermal renewable and non-renewable resources in virtual power plant, Int. J. Electr. Power Energy Syst. 11 (2021), 106658.
[20] S.Abrisham Foroushan Asl, L. Bagherzadeh, S. Pirouzi, M.A. Norouzi, M. Lehtonen, A new two-layer model for energy management in the smart distribution network containing flexi-renewable virtual power plant, Electr. Power Syst. Res. 194 (2021) 107085.
[21] M.M. Othman, Y.G. Hegazy, A.Y. Abdelaziz, Electrical energy management in unbalanced distribution networks using virtual power plant concept, Electr. Power Syst. Res. 145 (2017) 157–165.
[22] S.W. Park, S.Y. Son, Interaction-based virtual power plant operation methodology for distribution system operator's voltage management, Appl. Energy 271 (2020), 115222.
[23] Q. Yang, et al., Blockchain-based decentralized energy management platform for residential distributed energy resources in a virtual power plant, Appl. Energy 294 (2021), 117026.
[24] M. Shafiekhani, Optimal bidding strategy of a renewable-based virtual power plant including wind and solar units and dispatchable loads, Energy 239 (2022) 122379.
[25] S. Sadeghi, et al., Optimal bidding strategy of a virtual power plant in day-ahead energy and frequency regulation markets: a deep learning-based approach, Int. J. Electr. Power Energy Syst. 127 (2021), 106646.
[26] S. Yu, F. Fang, Y. Liu, J. Liu, Uncertainties of virtual power plant: problems and countermeasures, Appl. Energy 239 (2019) 454–470.
[27] A. Shahbazi, et al., Effects of resilience-oriented design on distribution networks operation planning, Electr. Power Syst. Res. 191 (2021), 106902.
[28] A. Shahbazi, et al., Hybrid stochastic/robust optimization model for resilient architecture of distribution networks against extreme weather conditions, Int. J. Electr. Power Energy Syst. 126 (2021), 106576.
[29] M.S. Khomami, K. Jalilpoor, M.T. Kenari, M.S. Sepasian, Bi-level network reconfiguration model to improve the resilience of distribution systems against extreme weather events, IET Gener. Transm. Distrib. 13 (2019) 3302–3310.
[30] V. Krishnamurthy, A. Kwasinski, Effects of power electronics, energy storage, power distribution architecture, and lifeline dependencies on microgrid resiliency during extreme events, IEEE J. Emerg. Sel. Top. Power Electron. 4 (2016) 1310–1323.
[31] S. Pirouzi, J. Aghaei, Mathematical modeling of electric vehicles contributions in voltage security of smart distribution networks, Simulation 95 (2018) 429–439.
[32] A. Rohani, et al., Bi-level power management strategy in harmonic-polluted active distribution network including virtual power plants, IET Renew. Power Gener. 15 (2021) 462–476.
[33] D. Bertsimas, E. Litvinov, X.A. Sun, J. Zhao, T. Zheng, Adaptive robust optimization for the security constrained unit commitment problem, IEEE Trans. Power Syst. 28 (2013) 52–63.
[34] A. Kavousi-Fard, A. Khodaei, Efficient integration of plug-in electric vehicles via reconfigurable microgrids, Energy 111 (2016) 653–663.
[35] S. Pirouzi, J. Aghaei, M.A. Latify, G.R. Yousefi, G. Mokryani, A robust optimization approach for active and reactive power management in smart distribution networks using electric vehicles, IEEE Syst. J. 12 (2017) 2699–2710.
[36] S. Katoch, S.S. Chauhan, V. Kumar, A review on genetic algorithm: past, present, and future, Multimed. Tools Appl. 80 (2021) 8091–8126.
[37] R.R. Rani, D. Ramyachitra, Krill Herd Optimization algorithm for cancer feature selection and random forest technique for classification, in: IEEE International Conference on Software Engineering and Service Science (ICSESS), Beijing, 2017, pp. 109–113.
[38] K. Sarwagya, P.K. Nayak, S. Ranjan, Optimal coordination of directional overcurrent relays in complex distribution networks using sine cosine algorithm, Electr. Power Syst. Res. 187 (2020), 106435.
[39] P.R. Babu, C.P. Rakesh, G. Srikanth, M.N. Kumar, D.P. Reddy, A novel approach for solving distribution networks, in: India Conference (INDICON), 2009Annual IEEE, 2009, pp. 1–5.
[40] W.K.A. Najy, H.H. Zeineldin, W.L. Woon, Optimal protection coordination for microgrids with grid-connected and islanded capability, IEEE Trans. Ind. Electron. 60 (2013) 1668–1677.
[41] S. Pirouzi, et al., Power conditioning of distribution networks via single-phase electric vehicles equipped, IEEE Syst. J. 13 (2019) 3433–3442.
[42] H. Kiani, et al., Adaptive robust operation of the active distribution network including renewable and flexible sources, Sustain. Energy Grids Netw. 26 (2021), 100476.
[43] M.R. Ansari, et al., Renewable generation and transmission expansion planning coordination with energy storage system: a flexibility point of view, Appl. Sci. 11 (2021) 3303.
[44] A. Dini, A flexible-reliable operation optimization model of the networked energy hubs with distributed generations, energy storage systems and demand response, Energy 239 (2022) 121923.
[45] A. Dini, et al., Security-constrained generation and transmission expansion planning based on optimal bidding in the energy and reserve markets, Electr. Power Syst. Res. 193 (2021), 107017.
[46] S. Arabi-Nowdeh, et al., Multi-criteria optimal design of hybrid clean energy system with battery storage considering off-and on-grid application, J. Clean. Prod. 290 (2021), 125808.
[47] A. Naderipour, et al., Deterministic and probabilistic multi-objective placement and sizing of wind renewable energy sources using improved spotted hyena optimizer, J. Clean. Prod. 286 (2021), 124941.
[48] S. Arabi Nowdeh , and et al. Fuzzy multi-objective placement of renewable energy sources in distribution system with objective of loss reduction and reliability improvement using a novel hybrid method. 20219, Appl. Soft Comput., Vol. 77, pp. 761-779.
[49] A. Naderipour, et al., Comparative evaluation of hybrid photovoltaic, wind, tidal and fuel cell clean system design for different regions with remote application considering cost, J. Clean. Prod. 283 (2021), 124207.
[50] A. Naderipour, et al., Hybrid energy system optimization with battery storage for remote area application considering loss of energy probability and economic analysis, Energy 239 (2022), 122303.
[51] S. Pirouzi, J. Aghaei, T. Niknam, H. Farahmand, M. Korpås, Exploring prospective benefits of electric vehicles for optimal energy conditioning in distribution networks, Energy 157 (2018) 679–689.
[52] H.S. Gill, B.S. Khehra, A. Singh, L. Kaur, Teaching-learning-based optimization algorithm to minimize cross entropy for selecting multilevel threshold values, Egypt. Inf. J. 20 (2019) 11–25.
[53] L. Ma, et al., Energy management for joint operation of CHP and PV prosumers inside a grid-connected microgrid: a game theoretic approach, IEEE Trans. Ind. Inf. 12 (2016) 1930–1942.
[54] W. Jiang, X. Wang, H. Huang, D. Zhang, N. Ghadimi, Optimal economic scheduling of microgrids considering renewable energy sources based on energy hub model using demand response and improved water wave optimization algorithm, J. Energy Storage 55 (2022), 105311.
[55] H.C. Nejad, S. Tavakoli, N. Ghadimi, S. Korjani, S. Nojavan, H. Pashaei-Didani, Reliability based optimal allocation of distributed generations in transmission systems under demand response program, Electr. Power Syst. Res. 176 (2019), 105952.
[56] D. Yu, N. Ghadimi, Reliability constraint stochastic UC by considering the correlation of random variables with Copula theory, IET Renew. Power Gener. 13 (2019) 2587–2593.
[57] S.A. Mansouri, E. Nematbakhsh, A. Ahmarinejad, A.R. Jordehi, M.S. Javadi, M. Marzband, A hierarchical scheduling framework for resilience enhancement of decentralized renewable-based microgrids considering proactive actions and mobile units, Renew Sust. Ener. Rev. (2022), https://doi.org/10.1016/j.rser.2022.112854.
[58] S.A.A. Matin, S.A. Mansouri, M. Bayat, A.R. Jordehi, P. Radmehr, A multi-objective bi-level optimization framework for dynamic maintenance planning of active distribution networks in the presence of energy storage systems, J. Ener. Storage (2022), https://doi.org/10.1016/j.est.2022.104762.
[59] S.A. Mansouri, A. Ahmarinejad, F. Sheidaei, M.S. Javadi, A. Rezaee Jordehi, A. Esmaeel Nezhad, J.P.S. Catalao, Int. J .Electr. Power Energy Syst (2022), https://doi.org/10.1016/j.ijepes.2022.
[60] M. Nasir, A. Rezaee Jordehi, S.A.A. Matin, V.S. Tabar, M. Tostado-Véliz, S. A. Mansouri, Optimal operation of energy hubs including parking lots for hydrogen vehicles and responsive demands, J. Ener. Storage (2022), https://doi.org/10.1016/j.est.2022.104630.
[61] M. Nasir, A.R. Jordehi, M. Tostado-Veliz, V.S. Tabar, S.A. Mansouri, F. Jurado, Operation of energy hubs with storage systems, solar, wind and biomass units connected to demand response aggregators, Sustain Cities Soc. (2022), https://doi.org/10.1016/j.scs.2022.103974.
[62] S.A. Mansouri, A. Ahmarinejad, E. Nematbakhsh, M.S. Javadi, A.R. Jordehi, JPS Catalão, Energy Hub Design in the Presence of P2G System Considering the Variable Efficiencies of Gas-Fired Converters, Int. Conf. Smart Energy Syst. Technol. (2021), https://doi.org/10.1109/SEST50973.2021.9543179.
[63] S.A. Mansouri, E. Nematbakhsh, M.S. Javadi, A.R. Jordehi, M. Shafie-khah, J.P. S. Catalão, Resilience Enhancement via Automatic Switching considering Direct Load Control Program and Energy Storage Systems, IEEE Int. Conf. Environ. Electr. Eng. (2021), https://doi.org/10.1109/EEEIC/ICPSEurope51590.2021.9584609.
[64] S.A. Mansouri, A. Ahmarinejad, E. Nematbakhsh, M.S. Javadi, A. Esmaeel Nezhad, J.P.S. Catalão, A sustainable framework for multi-microgrids energy management in automated distribution network by considering smart homes and high penetration of renewable energy resources, Energy (2022), https://doi.org/10.1016/j.energy.2022.123228.
[65] S.A. Mansouri, A. Ahmarinejad, E. Nematbakhsh, M.S. Javadi, A.R. Jordehi, J.P. S. Catalão, Energy Management in Microgrids including Smart Homes: A Multi-objective Approach, Sustain Cities Soc. (2021), https://doi.org/10.1016/j.scs.2021.102852.
[66] S.A. Mansouri, E. Nematbakhsh, A. Ahmarinejad, A.R. Jordehi, M.S. Javadi, S.A. A. Matin, Multi-objective dynamic framework for design of energy hub by considering energy storage system, power-to-gas technology and integrated demand response program, J Energy Storage (2022), https://doi.org/10.1016/j.est.2022.104206.
[67] S.A. Mansouri, A. Ahmarinejad, M. Ansarian, M.S. Javadi, J.P.S. Catalao, Stochastic planning and operation of energy hubs considering demand response programs

using Benders decomposition approach, Int. J. Electr. Power Energy Syst. (2020), https://doi.org/10.1016/j.ijepes.2020.106030.

[68] S.A. Mansouri, E. Nematbakhsh, A.R. Jordehi, M. Tostado-Véliz, F. Jurado, Z. Leonowicz, A Risk-Based Bi-Level Bidding System to Manage Day-Ahead Electricity Market and Scheduling of Interconnected Microgrids in the presence of Smart Homes, 2022 IEEE Int. Conf. Environ. Electr. Eng. 2022 IEEE Ind. Commer. Power Syst. Eur. (EEEIC / I&CPS Eur. (2022), https://doi.org/10.1109/EEEIC/ICPSEurope54979.2022.9854685.

[69] S.A. Mansouri, A. Ahmarinejad, M.S. Javadi, J.P.S. Catalão, Two-stage stochastic framework for energy hubs planning considering demand response programs, Energy 206 (2020) 118124, https://doi.org/10.1016/j.energy.2020.118124.

[70] S.A. Mansouri, M.S. Javadi, A. Ahmarinejad, E. Nematbakhsh, A. Zare, J.P. S. Catalão, A coordinated energy management framework for industrial, residential and commercial energy hubs considering demand response programs, Sustain Energy Technol. Assessments (2021), https://doi.org/10.1016/j.seta.2021.101376.